Energy 219 (2021) 119611

Contents lists available at ScienceDirect

Energy

journal homepage: www.elsevier.com/locate/energy

Estimation of photovoltaic power generation potential in 2020 and 2030 using land resource changes: An empirical study from China

Peng Wang [a, *], Shuainan Zhang [a], Yanru Pu [a], Shuchao Cao [b], Yuhu Zhang [c]

[a] Faculty of Civil Engineering and Mechanics, Jiangsu University, Zhenjiang, 212013, China
[b] School of Automotive and Traffic Engineering, Jiangsu University, Zhenjiang, 212013, China
[c] College of Resource Environment & Tourism, Capital Normal University, Beijing, 100048, China

ARTICLE INFO

Article history:
Received 2 May 2020
Received in revised form
6 December 2020
Accepted 12 December 2020
Available online 15 December 2020

Keywords:
PV generation Potential
Land resource change
Built-up area
Electricity consumption
Supply-demand nexus
Solar radiation

ABSTRACT

In this study, the future dynamic photovoltaic (PV) power generation potential, which represents the maximum PV power generation of a region, is evaluated. This study predicts suitable land resources for PV systems and calculates the PV generation potential based on these predictions. Then the supply and demand for PV power in the future is obtained by forecasting the future power consumption of the entire society. The results of this research showed that due to the influence of land resource changes, some provinces in China will have almost no PV generation potential in the year 2030. The gap between the PV potential of each province and future electricity consumption is closing, and the ratio of supply and demand is decreasing, which has been calculated to be 39.8 and 30.8 in 2020 and 2030, respectively, under the scenario of 100% PV power generation. This study reveals the influence of land resource changes on the PV power generation potential and provides a basis for other potential assessments that consider future socioeconomic development.

Author contribution

Peng Wang, Conceptualization, Methodology. Shuainan Zhang, Data curation, Software, Writing – original draft. Yanru Pu, Visualization, Investigation. Shuchao Cao, Validation, Writing-Reviewing and Editing. Yuhu Zhang, Supervision.

1. Introduction

Due to increased global warming and fossil energy depletion, the international community is paying increasing attention to the development and utilization of renewable energy [1–3]. Of all of the types of renewable energy sources, solar energy is regarded as the fastest growing energy due to its obvious advantages of being clean, safe, and inexhaustible [4,5]. China's PV market is developing rapidly to meet emission reduction standards due to policy support and continuous technological progress. The newly installed capacity of PV is increasing every year, from 0.02 GW in 2007 to 53.06 GW in 2017. By the end of 2017, China's PV installed capacity had reached 130.25 GW, accounting for 1.49% of the total power generation. Centralized PV facilities are the primary form of China's PV power generation application system. In 2018, compared with distributed PV, the cumulative installed capacity of centralized PV accounted for 71% [6]. Centralized PV power generation dominates the PV application market, and research regarding centralized PV development is of great significance.

However, there are many limitations that hinder the development of centralized PV. The availability of land resources is a factor that affects PV power development [4,5]. Compared with fossil fuels, solar energy is substantially more land intensive with regard to delivering the same amount of power. Fossil fuel energy consisting of concentrated deposits can be exploited at high power rates (200–11,000 W_e/m^2; W_e is electric power), while the net power density of a solar plant is 2–10 m^2 [8,9]. For some regions located in the northern latitudes with high population densities and high electricity consumption, policies that promote the development of a fossil fuel transition to renewable energy sources (RES)/solar will add pressure to land requirements. As the primary form of PV power generation, the demand for land resources of centralized PV systems would be substantial. In addition, the construction of a centralized PV system has strict land resource requirements [2,4,5,10]. Land resources for the construction of centralized PV systems need to meet some specific conditions,

* Corresponding author.
E-mail address: upeswp@ujs.edu.cn (P. Wang).

https://doi.org/10.1016/j.energy.2020.119611
0360-5442/

which include the global horizontal irradiance (GHI), the necessary slope required for centralized PV systems and the exclusion of unsuitable land types. In China, the suitable land area required for centralized PV systems in 2015 was estimated to be approximately 242.57 $\times$ 10^4 km^2, accounting for 25% of the country's total area [11].

In addition, the suitable area for PV construction are changing with socioeconomic development [5,10]. And the amount of solar radiation received by panels, which also affects PV generation, is changing. Changes in the amount of solar radiation are influenced by air pollution and associated aerosol loads, as well as their effects on clouds. It is an important signal reflecting climate change. According to Ref. [7], it can be known that the development of PV is relatively stable and when the change of solar radiation as the main factor to PV power generation is taken into account, the impact of such changes is relatively small. In addition, since this paper focuses on the impact of land change on PV power generation, the impact of solar radiation on PV power generation is not considered. From the perspective of land types, the area of unsuitable land use types has an important effect on suitable land resources. Specifically, with the rapid urban development, urban land areas cannot be ignored in regional land use projections [12]. Urban areas are regarded as one of the most affected land use types under the socioeconomic development scenario. The built-up area is an important indicator of urban area change and predicting the land resource demand for future urban development [13]. The expansion of the built-up area may lead to a significant reduction in suitable land resources. According to Zhang et al., the suitable area for PV development in China in 2015 was about 242.57 $\times$ $10^4 km^2$. Based on data from the 2018 China statistical yearbook, the total built-up area of 12 provinces in the study area was 2269.4 km^2 larger than the area in 2015, accounting for 0.1% of the suitable area. That means that the area suitable for PV development may be reduced by 0.1% in 2018. With the decreasing availability of land resources, the contradiction between limited land resources and the large land resource requirement for centralized PV system will be exacerbated in the future.

Therefore, considering the influence of socioeconomic development on the suitable land resources, it is necessary to evaluate the PV generation potential, which means the maximum amount of PV generation. In addition, with an increase in electricity consumption, more attention should be paid to the supply and demand of PV power generation in China. The potential evaluation of future dynamic PV generation will play an essential role in determining whether the power demand can be met and is essential in the planning of renewable energy development and distribution.

The study's largest innovation point is the evaluation of the future PV power generation potential, specifically taking into account the change of suitable area for laying PV panel due to changes in built-up area. Many studies are currently aimed at the past time node PV potential assessment, rarely assess the future potential. And these studies rarely consider the impact of socio-economic development on land resources suitable for laying PV panels. The second innovation point of the article is the method of calculating the PV generation potential. Compared with using GHI to represent the solar radiation absorbed by tilted PV panels and then to calculate the amount of electricity converted from solar radiation, the paper calculates the amount of solar radiation absorbed by tilting PV panel, which makes the results more accurate.

2. Literature review

In recent years, solar energy development and land resource uses have been found to be closely linked. This reflected in the impact of solar energy development on land use transformations and the environment. It is primarily due to the occupation of other land use types, such as cultivated land, and the indirect environmental impact [1,18,19]. It is also reflected in the relationship between the assessment of PV power potential and land resource uses. The connection is specifically reflected in the estimation of land requirements to meet PV power consumption and the assessment of PV generation potential based on suitable land resources [20,21,23–28].

In order to assess PV generation potential in a region more accurately, many studies improve the relevant indicators to identify suitable land area for PV construction. To solve the not yet reached consensus on land selection criteria in terms of the minimum GHI and maximum slope, Yang et al. used sensitivity analysis results to provide a more accurate indicator selection for assessment of generation potential [37]. Majumdar and Pasqualetti ranked the suitable area at different levels and estimated the generation potential under multiple decision-making scenarios [10]. Yue and Huang considered the requirements for the outstanding structural area on the roof as a proportion of the total area in the Building Code and make a general assessment of potential rooftop area available for installation of solar collectors [4]. But these articles only assess a certain period or point in time in the past and rarely predict the future PV generation potential.

In addition, social and economic factors are important constraints to take into account when evaluating solar energy potential. Particularly, land-use changes will have a significant impact on suitable sites for PV systems [5]. Rachchh et al. mentioned that the utilization of available space by urban areas is hindering the further growth of solar power [39]. He and Kammen mentioned that China's rapid urbanization in the context of the PV potential is necessary for an in-depth analysis [17]. Majumdar and Pasqualetti concluded that suitable areas for solar energy generation can become rapidly depleted due to conflicts with rapid urban growth [10]. But they have not discussed the changes in the PV potential based on this. To our greatest knowledge, only Gunderson et al. evaluated the PV potential in different situations of different availability of land resources in the Black Sea region [5]. However, the development situation in regions is various and it is necessary to assess the PV potential of a particular region according to local social development.

Research regarding the PV generation potential in China is in the initial stages. He and Kammen utilized 10-year hourly solar irradiation data from 2001 to 2010 obtained from 200 representative locations to estimate the PV generation potential of different solar technologies [17]. Yang et al. considered the land conversion coefficient of PV construction and comprehensively evaluated the current power generation potential of China [37]. Xu et al. considered the role of technological progress of PV development, and simulated the path for solar power under different development scenarios [38]. Considering the accuracy of data, the land conversion of PV construction and technological progress, the assessment of the PV potential in China was more accurate. However, currently there exist few studies that have investigated the changes in the PV power potential under the scenarios of China's future social-economic development, particularly with the changes in available land resources caused by urban development.

Therefore, the study will consider the impact of land resource changes on the PV generation potential in China in the context of social-economic development and evaluate the potential based on this. The main content of the article is to evaluate the PV potential in 2015, and then predict the potential in 2020 and 2030 based on different development scenarios. This not only complements the relevant studies to assess the future PV potential, but also confirms the changes in PV potential due to changes in land resources under social-economic development scenarios.

The paper is organized as follows: Section 3 describes the research area and data sources. Section 4 details the calculation method of the PV generation potential and prediction of the future potential and electricity consumption. Section 5 details the results and provides a discussion. Finally, section 6 outlines the primary conclusions and provides policy recommendations.

3. Study area and data

3.1. Study area

The primary premise for determining the study area was to select land resources suitable for PV system development. In this study, the suitable PV area selection result of Zhang et al. was referred to because this study considered the suitable conditions for the PV construction more comprehensively and accurately. The relevant data results are shown in Fig. 1 and Table 1. For convenience in the subsequent calculation, this study roughly selected the grid points shown in Fig. 1 that are distributed on the suitable area basically. In addition, the province where all of the grid points are located was used as the research object. These were Xinjiang, Gansu, Qinghai, Ningxia, Shaanxi, Inner Mongolia, Hebei, Shanxi, Shandong, Fujian, Tibet, and Sichuan.

The suitability referred in this paper focuses on local natural conditions, representing the nature of solar panels can be laid if the laying requirements and the absorption of solar radiation can be satisfied. Therefore, the suitability of the land for solar panels is not taken into account the technical and policy factors.

Land areas suitable for the PV construction need to satisfy three aspects, which conclude geographic constraints, the solar radiation threshold and elimination of unsuitable land types. Specifically, the locations with a slope of more than 5° are not suitable for laying solar panels and areas with solar radiation below 5400 MJ/m^2 were generally considered unsuitable areas. And there are six land use patterns unsuitable for the PV construction, including protected areas, water bodies, cultivated land, forest land, high-coverage grasslands, and construction lands. The rationality of these selection criteria is described in detail below.

The election of land types mainly refers to other literature and is principally based on the minimization of the possible environmental impact derived from the construction of future PV power plants [40]. For example, the urban areas were unsuitable due to the high density of population and buildings and traffic safety issues [41]. And protected areas which plays an important role in keeping the balance of nature are not suitable for the construction of large-scale PV plants [37]. About the setting of the minimum slope, flat areas or mild steep slopes will help to avoid the high construction cost required in high slope areas. Based on the data from various literary works, the slope factor for this study should be less than or equal to 5° [41,42]. About the setting of the minimum amount of solar radiation, there has been no consensus regarding the minimum acceptable radiation for large-scale PV power plants. In this study, 5400 MJ/m^2 was chosen as the baseline.

Based on the results from Ref. [11], the study identified the research area, and then selected the 12 provinces to which the research area belongs as the research object. This scale was chosen due to the spatial heterogeneity of solar energy development, which contained three directions: scale of development, direction of development and status quo.

According to the Solar power development "13th Five-Year Plan", the scale of PV construction planned in different provinces vary in 2020, such as 12 million kilowatts in Inner Mongolia, Shanxi and Hebei and 6 million kilowatts in Anhui and Guangdong [43]. In addition, with comprehensive consideration of solar energy resources, grid access, land use conditions and other effects, the provincial PV development plan is different. Qinghai, Inner Mongolia and other areas with rich solar energy and abundant land resources are encouraged in the construction of solar power and other renewable energy complementary power base while the Northeast and North China are encouraged to actively promote the integration of solar and conventional energy and adopt a centralized and distributed combination of the way of building heating. Besides, the current situation of PV development is different in each province. Judging from the new installation layout, in 2019, 8.58 million kilowatts were installed in North China, accounting for 28.5% of the country's total, while 1.53 million kilowatts were installed in Northeast China, accounting for 5.1%; From the key regions, PV emission problems mainly appear in the northwest region, its waste light accounted for 87% of the country. From the key provinces, Tibet, Xinjiang, Gansu waste light rate of 24.1%, 7.4%, 4.0%, respectively [35].

3.2. Data

The statistical data involved in the evaluation of the PV generation potential included solar radiation and the elevation. The solar radiation dataset used in this study was the ERA-Interim meteorological reanalysis data provided by the European Centre for Medium-Range Weather Forecasts (ECMWF). This study selected the solar radiation dataset that covered all of the provinces of China from January 1, 1979 to December 31, 2017 with a spatial resolution of 0.75 ° × 0.75 °. The value selected for this study was the annual average solar radiation from 1979 to 2017. In addition, this study assumed that the radiation data of each grid point represented the average amount of solar radiation in a grid centered at 0.75 ° × 0.75 °. The elevations of the coordinate points were obtained from the SRTM3 digital elevation data. Prior to obtaining the elevation data, specific information regarding the location of the grid point was identified using ArcGIS according to a 0.75 ° × 0.75 ° spatial resolution of the solar radiation data map.

The analysis of land changes and the social power consumption required the data of the gross domestic product (GDP) per capital, the urbanization rate, the built district area, population, the value-added of each industry, and GDP. GDP per capital, built district area, population, the value-added of each industry, and GDP of the 12 provinces from 2010 to 2019 were acquired from the China Statistical Yearbook. The level of urbanization was the proportion of urban population to the total population, and the percentage of the urban population data in 2009–2019 was acquired to calculate the percentage of the urban population changed from the last year in 2010–2019.

4. Methods

Fig. 2 **s**hows a summary of the study methodology flow. The PV generation potential based on the suitable area in 2015 was evaluated, and then the potential in 2020 and 2030 were estimated by predicting the change in the built-up area compared with that in 2015. The future electricity consumption was forecasted and compared with the generation potential. Figs. 3 and 4 **s**hows the calculation of provincial PV generation potential and the solar radiation by tiled panels.

In the data section, it has been stated that this study assumes that the solar radiation data represents the average solar radiation intensity in a grid of 0.75 ° × 0.75 ° with the grid point as the center. Therefore, coinciding with the spatial range of the solar radiation data, the generation potential was calculated for a single grid. Then the potential of a province was obtained by screening and summing the grid's potential.

4.1. Maximum PV power generation in a grid

To evaluate the maximum PV power generation, there were two conditions required for calculation: (1) all of the solar panels are laid on the suitable area (2) each panel receives the largest inclined solar radiation calculated at noon of the summer solstice with the best tilt angle.

4.1.1. Determining the tilt angle

Tilt angle tends to be 0° laying PV panels around the equator is more common, because the direct sunlight around the equator is frequent and PV panel can obtain sufficient solar radiation. But tiled PV panels are not suitable for other latitudes. For grid-connected ground PV systems, the target is usually to harvest the highest possible irradiation during the year to maximize yearly PV generation. The optimal tilt angle is determined to achieve this goal [29]. China's geographical location determines that the laying of PV panels should have a certain tilt angle. In addition, the laying of PV panels should reduce the cost to achieve economic feasibility and consider the convenience of daily cleaning panels [14]. It is clear that closely laying PV panels in a flat form may not feasible in economic, PV panel installation clean-up and so on compared with laying PV panels at a certain tilt angle with front and rear spacing.

The latitude Φ is the most determinant variable among various influencing factors of the optimum tilt angle β_{opt}. Although the local climate conditions at each site affect the optimization of the tilt angle, the latitude is the most determinant variable [29]. At the same time, the fitting value of the best tilt angle calculation formula referenced in this paper is 99.3%, thus the paper regards latitude as the variable to determine the optimal tilt angle.

$$\beta = -0.0049\Phi^2 + 1.0888\Phi \quad (1)$$

4.1.2. Solar radiation on an inclined surface

The calculation of the amount of solar radiation on an inclined surface was divided into the following six parts: a) Earth's declination δ; b) hour angle ω; c) solar elevation angle h; d) air quality m; e) atmospheric transparency factor P; and f) solar radiation on an inclined surface I_T.

During the summer solstice, the northern hemisphere receives most of the solar radiation. The Earth's declination δ was then calculated using the equation that used the summer solstice (June 21st, $n = 173$) to calculate the maximum amount of solar radiation received by the PV panels:

$$\delta = 23.45 \sin[360^\circ(284+n)/365] \quad (2)$$

In addition, the hour angle ω was calculated from the following equation, where t is the time ranging from 0 to 24 h. The solar altitude angle is the largest and the solar radiation is the strongest at midday, and this study used t to 12 to calculate the maximum amount of solar radiation:

$$\omega = 15(t-12) \quad (3)$$

The solar elevation angle h was calculated from the earth's declination δ, the latitude Φ and the hour angle ω:

$$\sin h = \sin\Phi \sin\delta + \cos\Phi \cos\delta \cos\omega \quad (4)$$

The calculation of the air quality m used two cases: when the sun elevation was 30° or more and less than 30°. Based on the calculation of the solar elevation angle at every latitude in the study area, the cases where sun elevations were all 30° or more in the area were selected. Then the air quality m was calculated using one of the following formulas [13]:

$$m = 1/\sin h \quad (5)$$

The expression for the atmospheric transparency factor P was obtained from $P(z)/P_0$, $m(z,h)$ and P (Equation (6), (7), and (8)), where $P(z)/P_0$ is the atmospheric pressure correction factor; $m(z,h)$ is the revised atmospheric quality and L is the height. This study used the atmospheric transparency factor for direct radiation to represent the total radiation's P [13].

$$P(z) \Big/ P_0 = [(288 - 0.0065L)/288]^{5.256} \quad (6)$$

$$m(z,h) = m \times P(z)/P_0 \quad (7)$$

$$P = 0.56\left(e^{-0.56m(z,\,h)} + e^{-0.096m(z,\,h)}\right) \quad (8)$$

The total horizontal radiation I is composed of the direct radiation I_{DH} and scattering I_{dH}.

$$I_{DH} + I_{dH} = I \quad (9)$$

I_{DH} and $I_{dH}$are expressed as follows:

$$I_{DH} = I_0 \times P^m \times \sin h \quad (10)$$

$$I_{dH} = 1/2 \times I_0 \times \sin h \times (1 - P^m)/(1 - 1.4 \ln P) \quad (11)$$

where I_0 is solar constant.

It is worth noting that the solar constant I_0 changes every year, and the value of the solar radiation intensity used was from 1979 to 2017. Therefore, the calculation result of the direct radiation and scattering obtained by the above Equations (10) and (11) was not inaccurate, and the direct radiation and scattering was calculated using a ratio of the two. The ratio of direct radiation and scattering R is:

$$R = (1 - P^m)/[2 \times P^m \times (1 - 1.4 \ln P)] \quad (12)$$

By combining Equations (9) and (12), I_{DH} and I_{dH} could be calculated separately.

By considering the equation of the above expressions, the amount of solar radiation on an inclined surface I_T with an inclination angle β may be expressed as a function of the direct radiation I_{DH}, scattering I_{dH}, total horizontal radiation I, the ground reflectanceρ, the optimum tilt angle β_{opt}, and the ratio R_b. Among of these factors, ρ is typically approximately 0.2, and this study used 0.2 as the constant [30]:

$$R_b = \frac{[\cos(\Phi - \beta_{opt})\cos\delta\cos\omega + \sin(\Phi - \beta_{opt})\sin\delta]}{(\cos\Phi\cos\delta\cos\omega + \sin\Phi\sin\delta)} \quad (13)$$

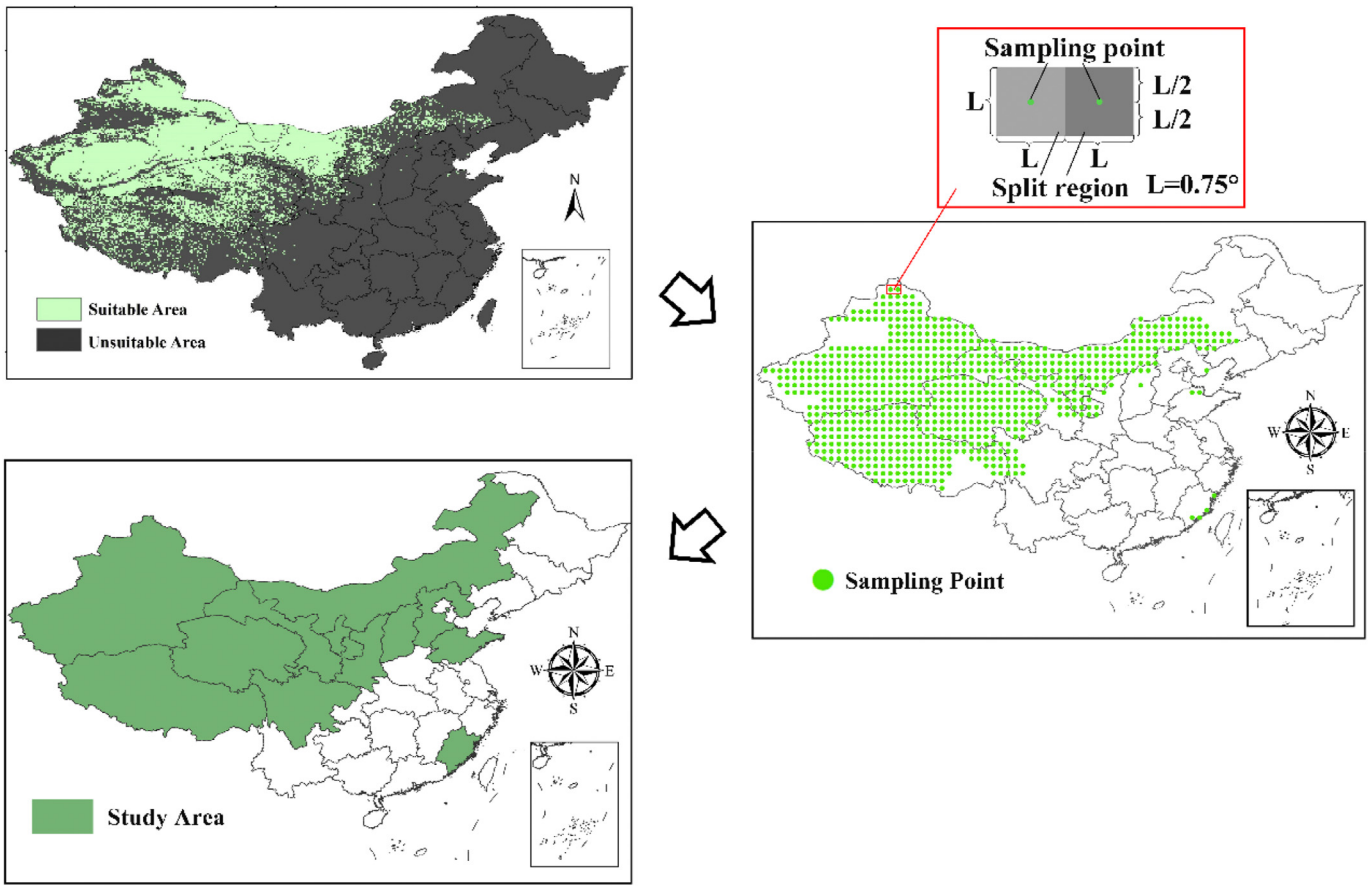

Fig. 1. Study area and selected grid points.

Table 1
Suitable area of 12 provinces.

Province	Total area (10^4 km^2)	Suitable area (10^4 km^2)
Hebei	19.79	0.06
Shanxi	16.02	0.08
Inner Mongolia	135.07	39.30
Fujian	11.15	0.02
Shandong	15.64	0.12
Sichuan	45.44	0.78
Tibet	113.94	28.01
Shaanxi	20.41	0.52
Gansu	41.41	19.07
Qinghai	71.53	36.72
Ningxia	5.21	1.60
Xinjiang	176.22	116.29

$$I_T = I_{DH} \times R_b + 1/2 \times I_{dH} \times (1 + \cos\beta_{opt}) + 1/2 \times \rho \times I \times (1 - \cos\beta_{opt}) \quad (14)$$

4.1.3. Minimal footprint of individual solar panels

To obtain the maximum solar panels area in the suitable region, it was necessary to calculate the minimum area occupied by the solar panels. This is related to the minimum distance between the front and back of the panel arrangement. The layout of the panels should consider the system loss percentage due to shading. Since the winter solstice has the longest shadow for objects in the Northern Hemisphere, the minimum distance, d, between arrays was calculated as the following formulas, and the schematic diagram of the solar panels representing the winter solstice is shown in the figure below (Fig. 5):

$$d = l\cos\beta_{opt} + (l \sin\beta_{opt}) / \tan(66,55 - \Phi) \quad (15)$$

where l is the width of the solar panel ($l = 1$m); β_{opt} is the optimum tilt angle; and Φ is the latitude.

The area of the land occupied by one solar panel were obtained as follows (The solar panel is 2 m long):

$$A = 2 \times d \quad (16)$$

4.1.4. Maximum solar panel area under different grids

To evaluate the generation potential under the actual area, the square of 0.75 ° × 0.75 ° needed to be converted to the actual geographical area. The latitude across the meridian was equivalent to 111 km of the actual geographic area, and the distance of one degree of latitude across the latitude was equivalent to the product of 111 km of the actual geographic area and the cosine of that

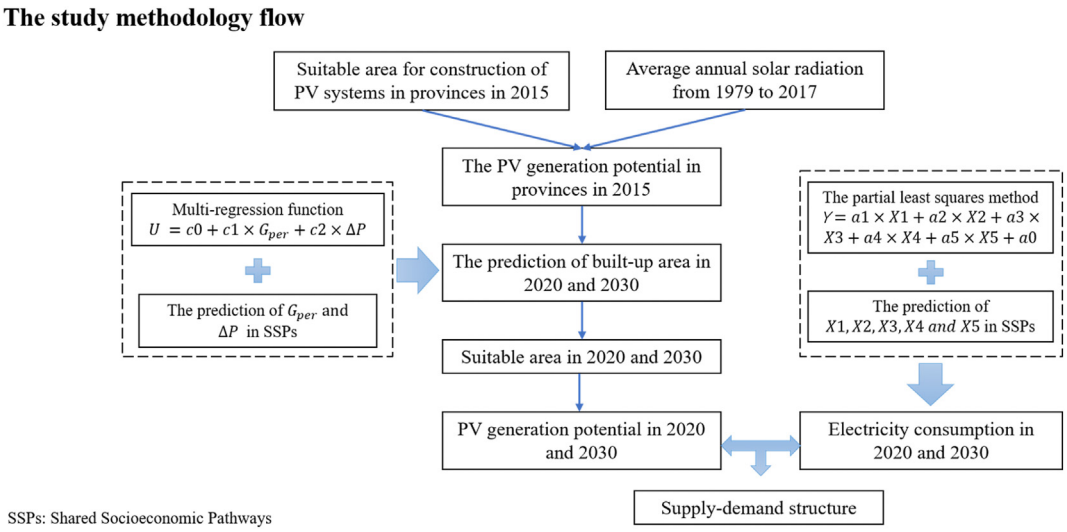

Fig. 2. The study methodology flow.

latitude. While on actual land, one grid represented different areas, and the specific calculation is shown as follows:

$$A_r = 111 \times 0.75 \times 111 \times 0.75 \times \cos \Phi \quad (17)$$

where A_r is the real land of a grid; and Φ is the latitude.

Under the condition that all of the solar panels are to be laid on this area, the panel laying area was calculated as follows:

$$A_a = A_r \times 1/A \times 2 \quad (18)$$

4.1.5. PV power generation of a grid

The expression for PV generated potential E_{PV} becomes [29]:

$$E_{PV} = \eta \times A_a \times I_T \times PR \times (1 - F_S) \quad (19)$$

where A_a is area of the laying panels on a grid; η is the PV module efficiency; the PR (performance ratio) is the ratio of the final system yield to the reference yield; and the F_S is the shading factor. This study assumed that the performance conditions were the same in all of the cases for simplification (η=15%, $PR = 0.8$,$F_S = 0.05$).

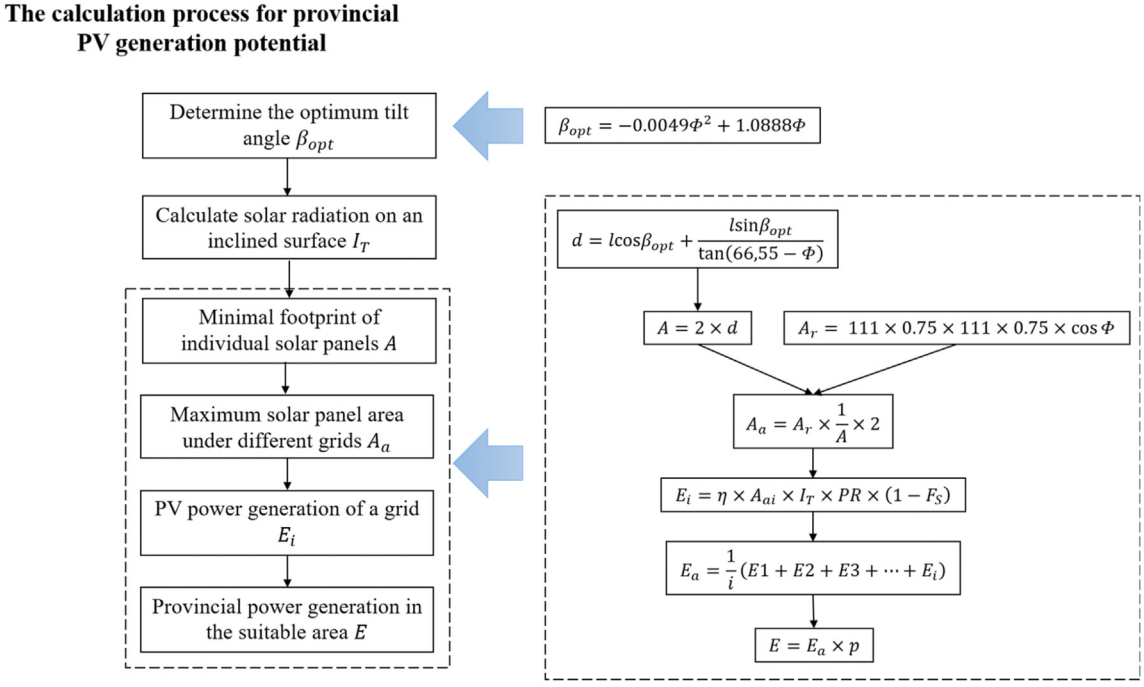

Fig. 3. Specific steps to calculate provincial PV generation potential.

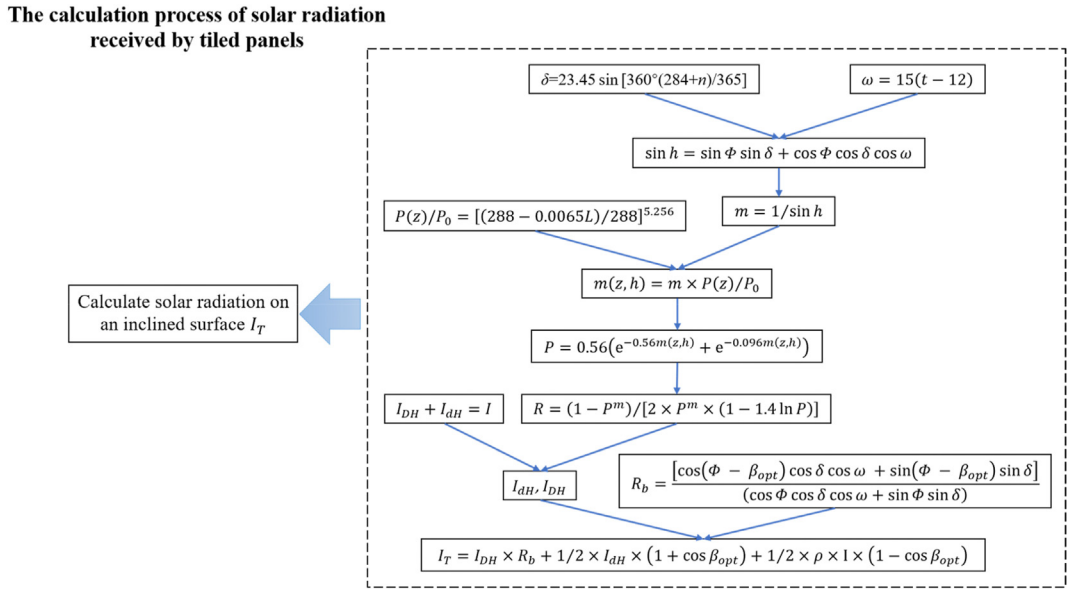

Fig. 4. Specific steps to calculate solar radiation received by tiled panels.

4.2. Provincial power generation in the suitable area

As Fig. 1 shows, the points in each province were selected according to the most suitable area of each province. Then the average PV potential in the selected grids in a province E_a is calculated using Equation (21). Based on E_a and the ratio of suitable area to the average area of the selected grids p, PV generation potential in the province E was obtained. The specific equations are as follows:

$$E_i = \eta \times A_{ai} \times I_T \times PR \times (1 - F_S) \tag{20}$$

$$E_a = 1 / i \times (E1 + E2 + E3 + \ldots + E_i) \tag{21}$$

$$E = E_a \times p \tag{22}$$

where i is the number of selected points in a province and E_i represents the PV generation potential of a grid centered on the selected point.

In order to make the method of calculating PV potential suitable for other geographical regions, it can be improved from some aspects. For the southern hemisphere, the number of date series in a year n need to be set to the winter solstate. Besides, the minimum front and rear spacing of PV panels should be based on the summer solstate calculation results. What's more, regions with different urbanization development may use different explanatory variables when predicting the construction area and electricity demand in the future. And predictions such as future PV power potential should be based on particular socio-economic development scenarios.

4.3. Varying solar panel laying areas

4.3.1. Regression equation of the built-up area

The GDP per capital and urban population changes have been found to be the two most fundamental drivers of urban development, and they have strong positive correlations [31]. Therefore, a multi-regression function could be built among the built-up areas, GDP per capital and urban population changes using statistical data from 2009 to 2018. The expressions are shown as follows:

$$U = c0 + c1 \times G_{per} + c2 \times \Delta P \tag{23}$$

where U is the built-up areas; G_{per} per is the GDP per capital; and ΔP indicates the proportion of urban population to total population changed from the same period last year.

4.3.2. Prediction of the future built-up area and PV power generation

Setting up a single scenario is an important reason for inaccurate forecast results and the reliable data of future socioeconomic scenarios is crucial [15]. The study will forecast the future electricity consumption and PV potential under the five scenarios of Shared Socioeconomic Pathways (SSPs). Predictive results of SSPs indicate that the future PV potential and electricity consumption are within a certain range. This not only reduces the uncertainty of the forecast results but provides richer reference for planning future PV development. The description of the SSPs is shown in Table 2.

According to the relevant research, the urbanization rate and GDP of each province are based on the data available in 2018 and the forecasts growth rate in 2020. Population and industrial output value are based on China's future projections and the proportion of provinces. Per capital GDP is the ratio of GDP to population [16,22,32,33]. The projected results built-up area, suitable area for PV construction and PV generation potential in SSPs can be found in Supplementary Table 1, 2, 3.

4.4. The entire social electricity consumption

4.4.1. Regression equation for the electricity consumption

The annual electricity consumption is affected by population, GDP and the first, the second and third production values [34]. There exist significant multiple correlations between these factors and electricity consumption. The partial least square method overcomes this problem. Based on the relevant data from 2010 to 2018, the regression equation used the partial least squares method are as follows:

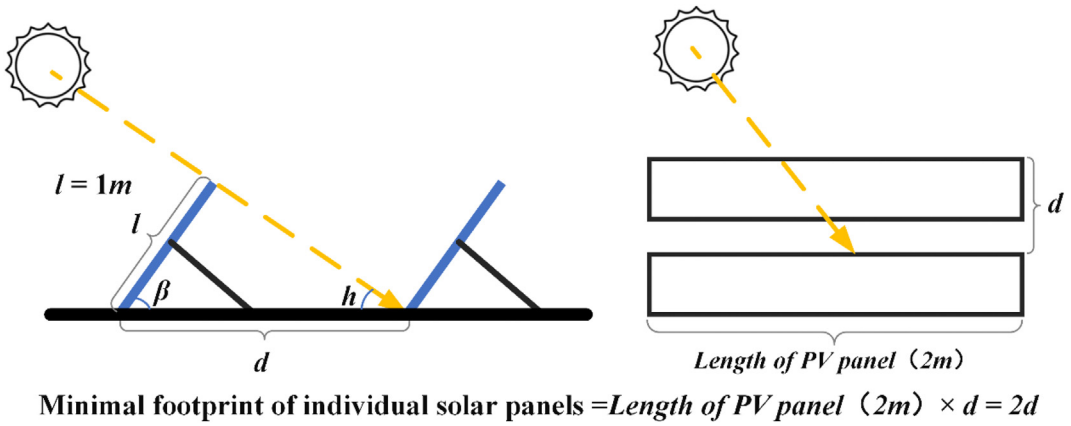

Fig. 5. Minimum distance needed between panels and minimal footprint of single panel.

$$Y = a1 \times X1 + a2 \times X2 + a3 \times X3 + a4 \times X4 + a5 \times X5 + a0 \quad (24)$$

where Y is the entire social electricity consumption; $X1$ is the population; $X2$ is the increased output value of the primary industry; $X3$ is the increased output value of the second industry; $X4$ is the increased output value of the tertiary industry; and $X5$ is the GDP.

4.4.2. Prediction of electricity consumption and its influencing factors

In the same way as the method of predicting urbanization rate mentioned in the 4.3.2., the population, industrial output value and GDP is predicted under different scenarios. The projected results of electricity consumption in SSPs can be found in Supplementary Table 4.

5. Result

5.1. Expansion in the built-up area and prediction of the PV generation potential

This study will provide an important introduction to the results under the SSP1 scenario. The results of other scenarios have similar characteristics and differences in results under five scenarios are discussed in 5.3.

As Table 3shown, the expansion of the built-up areas in some provinces has directly led to a sharp decline in the suitable area. In Shandong and Hebei, compared with 2015, the built-up area in 2030 increased by approximately 115.32% and 66.7%, respectively, which lead to almost no suitable area. In contrast, the change in the built-up area in some provinces caused a small reduction in the suitable area. In Tibet, Qinghai, Inner Mongolia, Xinjiang, and Gansu, the suitable areas in 2020 and 2030 were reduced by approximately 0.1% compared with that in 2015 although the changes in the built-up areas were relatively large.

Figs. 6 and 7 show the PV generation potential of the 12 provinces in 2020 and 2030. It can be seen that the PV potential in China is generally high in the western region accounted for in 86% and low occupied 0.01% in the eastern region. Specifically, Xinjiang, Qinghai, and Tibet in the western region accounted for a large proportion, which was 45%, 17%, and 15% both in 2020 and 2030 (see Table 4). The potential in Inner Mongolia accounted for 13% of the 12 provinces, which is a principal part of the PV potential in the north. From the time dimension, the PV potential of the 12 provinces decreased to different degrees from 2020 to 2030. In Xinjiang, the generation potential in 2030 is only 0.05% less than that in 2020. However, the potential of Fujian, Hebei, Shanxi, Shandong, Shaanxi, and Sichuan in 2020 and 2030 were significantly reduced compared with 2015. Specially, in Fujian, Hebei, and Shandong there was little potential for PV generation in 2030.

5.2. Prediction of electricity consumption

From 2020 to 2030, except Tibet, the electricity consumption of the 11 provinces will increase by a large margin, which is more than 15%. In particular, Shandong, Xinjiang and Shaanxi Province have relatively large increase in electricity consumption, which is 87%, 59% and 42%, respectively. From the spatial dimension, the electricity consumption in the northern and eastern regions of China will be larger than that in the western regions (see Figs. 8 and 9). The electricity consumption in the north and east accounted for 65% in the 12 provinces. Among these provinces, Shandong accounted for approximately 23% and 30% in 2020 and 2030, which is the most electricity-using province among the 12 provinces. Tibet showed the smallest electricity consumption in 2020 and 2030, accounting for 0.22% and 0.16% (see Table 5).

5.3. Supply and demand comparison of PV power generation

As shown in Figs. 10 and 11, the supply and demand situation of

Table 2
SSPs (1–5) and descriptions.

Scenarios	Description
SSP1	A sustainable path, with relatively high-speed technology transformation and policy support
SSP2	An intermediate path, maintaining the current pace of development
SSP3	A regional competitive path, with each country focused on its own energy and food security
SSP4	An unbalanced path. Large numbers of poor groups in industrialized and developing countries are vulnerable to climate change
SSP5	A fossil fuel-based development path that brings a lot of greenhouse gas emissions and faces significant mitigation challenges

Table 3
Built-up area in 2020 and 2030 in SSP1.

Provinces	Suitable area in 2015 (km^2)	2020		2030	
		Increase in built-up area compared to 2015 (%)	Reduction in suitable area compared to 2015 (%)	Increase in built-up area compared to 2015 (%)	Reduction in suitable area compared to 2015 (%)
Hebei	600	10.15	32.91	66.37	100
Shanxi	5200	25.44	35.73	34.29	48.16
Inner Mongolia	393000	1.05	0	6.83	0.02
Fujian	200	17.69	100	51.30	100
Shandong	1200	23.69	91.00	115.32	100
Sichuan	7800	37.80	11.06	118.21	34.58
Tibet	280100	28.63	0.01	38.93	0.02
Shaanxi	800	37.68	7.78	114.60	23.66
Gansu	190700	14.50	0.06	58.84	0.26
Qinghai	367200	19.04	0.01	63.86	0.03
Ningxia	16000	13.15	0.37	44.35	1.26
Xinjiang	1162900	22.74	0.02	69.93	0.07

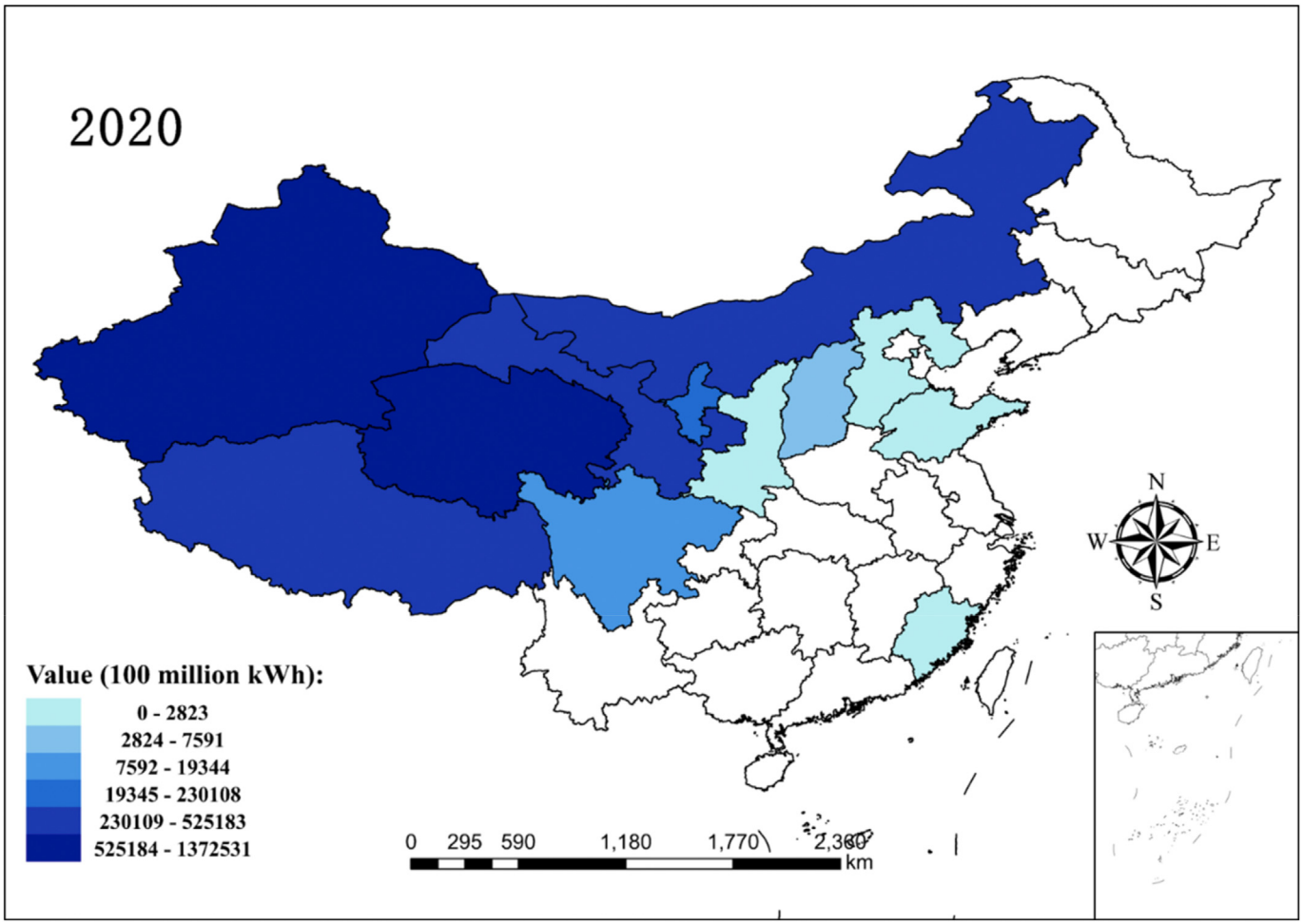

Fig. 6. PV power generation potential in 2020 in SSP1.

PV power in China is characterized by a serious imbalance and spatial heterogeneity. The supply and demand for PV in 12 provinces is primarily divided into two categories.

One is the optimistic situation that PV generation potential will be able to meet the demand for electricity. This scenario primarily applies to the western region, except Shaanxi. In the western region, generation potential in Tibet, Qinghai, Xinjiang, and Gansu is far greater than the electricity demand, and the supply-demand ratios are projected to be 7392, 752, 392 and 147 in 2030, respectively. Particularly, although Xinjiang is predicted to have large electricity consumption in the next decade, the supply and demand situation is optimistic due to the significant PV potential. The other is the pessimistic situation where the PV generation potential located cannot meet the demand for electricity. For example, in Shandong, Fujian, and Hebei, the PV power generation will no longer meet the larger power demand of the province in 2020.

From the time dimension, the ratio of PV generation supply to

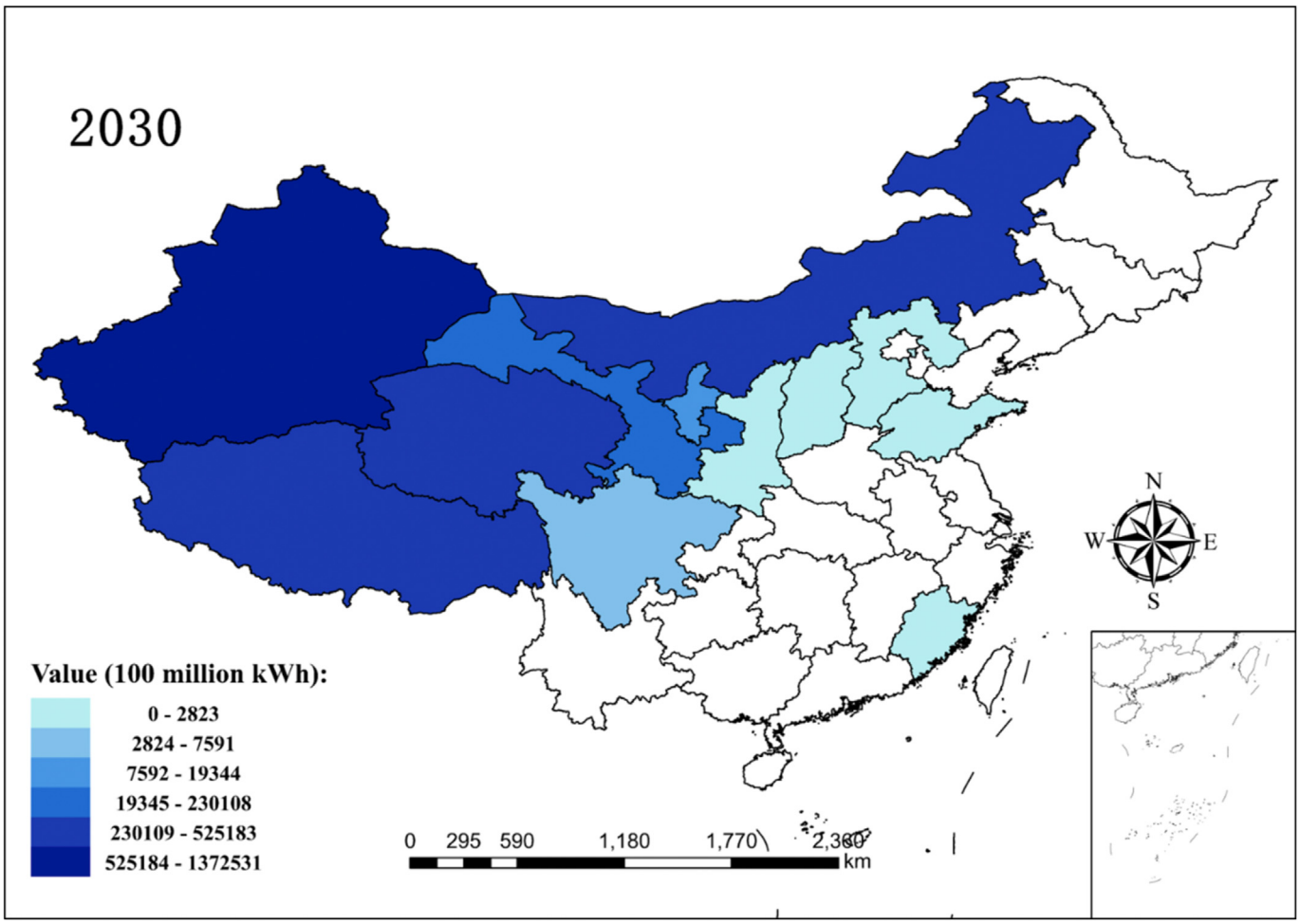

Fig. 7. PV power generation potential in 2030 in SSP1.

Table 4
The prediction of PV generation potential in SSP1.

Physical Geographic Division	Province	2020		2030		PV generation potential decreases in 2030 compared with 2020 (%)
		PV power generation potential (100 million kWh)	Proportion of nation power generation potential (%)	PV power generation potential (100 million kWh)	Proportion of nation power generation potential (%)	
North China	Hebei	400.77	0.01	0	0	100.00
	Shanxi	3499.59	0.12	2822.747333	0.09	19.34
	Inner Mongolia	407597.26	13.46	407523.7788	13.48	0.02
East China	Fujian	0	0	0	0	
	Shandong	117.01	0	0	0	100.00
West China	Sichuan	10319.33	0.34	7590.322996	0.25	26.45
	Tibet	457118.73	15.10	457094.4304	15.12	0.01
	Shaanxi	847.23	0.03	701.349597	0.02	17.22
	Gansu	230555.43	7.61	230107.9137	7.61	0.19
	Qinghai	525306.73	17.35	525182.1573	17.38	0.02
	Ningxia	19517.37	0.64	19343.49427	0.64	0.89
	Xinjiang	1372530.16	45.33	1371869.885	45.39	0.05
Sum		3027809.61	100	3022236.08	100	0.18

demand in the 12 provinces will decrease from 2020 to 2030, as shown in Table 6. This reveals that during the expansion of built-up areas and the growth of social electricity consumption, the gap between PV power generation and electricity consumption will gradually decrease. PV power generation in the future may not be able to meet the demand for social electricity consumption.

5.4. PV generation potential and electricity consumption in SSPs

As Fig. 12 (a) shown, with the exception of the SSP3 and SSP4 scenarios in Hebei, which changed by 35% and 11% compared to the SSP1 scenarios, the SSP1 scenarios in other provinces changed by less than 4%. Shandong and Fujian are not shown in Fig. 12 (a) because of the large changes of PV potential in SSPs. Specifically, the

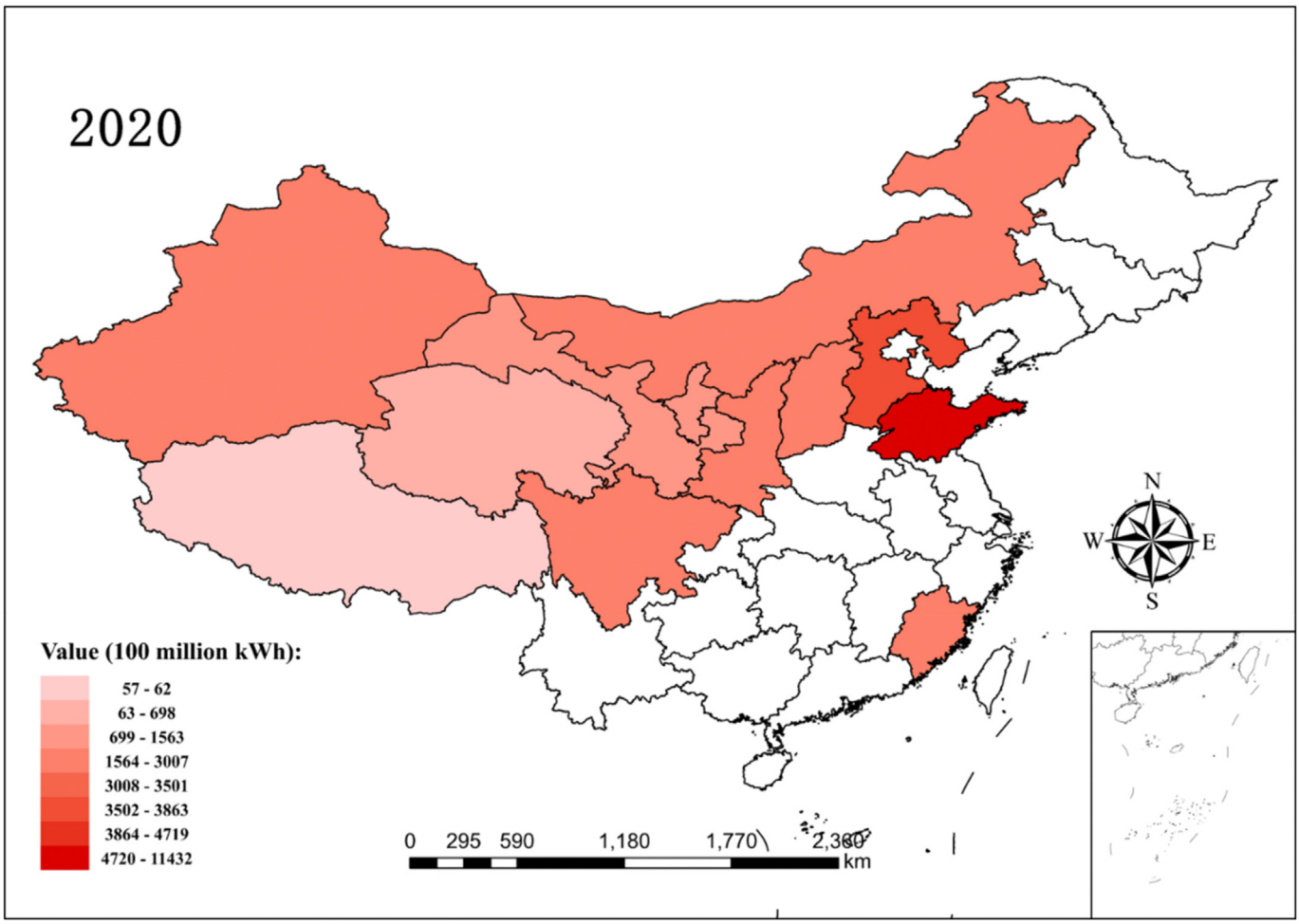

Fig. 8. Electricity consumption in 2020 in SSP1.

potential of Shandong in the SSP2 and SSP3 increased by about 300% compared to SSP1. The potential in Fujian in SSP3 is forecast to be 3.2 TWh (1 TWh = 109 kWh) while in other scenarios that is close 0.

As Fig. 12 (c) shown, the potential value of Shaanxi, Sichuan and Shanxi in SSP3 and SSP4 has changed by 30% and 20% compared to SSP1, while the potential of other provinces has not changed significantly under different scenarios. Since the PV potential of Hebei, Fujian and Shandong is close to 0 in SSPs in 2030, the three provinces are not represented in Fig. 12 (c).

Compared with the generation potential, the electricity consumption in 12 provinces changed more evenly under SSPs (Fig.12 (b) and (d)). As Fig. 12 (b) shown, the electricity consumption value of 12 provinces in the SSP3 scenario decreased by about 4% compared to SSP1 in 2020. Under SSP4, the potential value of Qinghai and Tibet increased by 8% and 4% compared to SSP1, respectively, and decreased by 4% in Shandong. Besides, other provinces vary by less than 4% in SSPs.

As Fig. 12 (d) shown, in 2030, all provinces are predicted to consume about 30% less electricity in the SSP3 than in the SSP1. Under the SSP5 situation, the power consumption in Shandong, Fujian and Tibet changed by more than 12% compared to SSP1. And under the SSP4 situation, the power consumption in Xinjiang, Shaanxi, Shandong and Shanxi changed by more than 18%. Shandong, of all provinces, had the largest change in electricity consumption under different conditions.

From the view of supply and demand, the difference between supply and demand has changed to varying degrees in SSPs. (Supplementary Table 5). Except for Hebei, Shanxi, Fujian, Shandong and Shaanxi, the gap between supply and demand in the other provinces is within 5% of the change compared to the SSP1 under SSPs in 2020 and 2030. In addition, the supply and demand relationships in all provinces except Shanxi are the same under SSPs. For example, PV potential supply of Hebei in 2020 and 2030 is always less than the demand for electricity and supply of Xinjiang is always more than the demand. However, in Shanxi, PV potential supply are not able to meet the demand for electricity in 2030 in SSP1 while in the other SSPs the supply is greater than the demand.

6. Discussion

6.1. Future PV generation potential

The reduction of PV generation potential is closely related to the expansion of the built-up area. As a significant reflection of anthropogenic activities, urbanization levels displayed ascending trends in the coastal provinces, such as Fujian Province. Due to the coordinated development strategy for Beijing, Tianjin, and Hebei, the long-term development trend of Hebei Province is very optimistic. Urban and economic development has led to the large-scale growth of the built-up areas in these areas. In addition, because Fujian and Hebei Provinces have large agricultural outputs, with

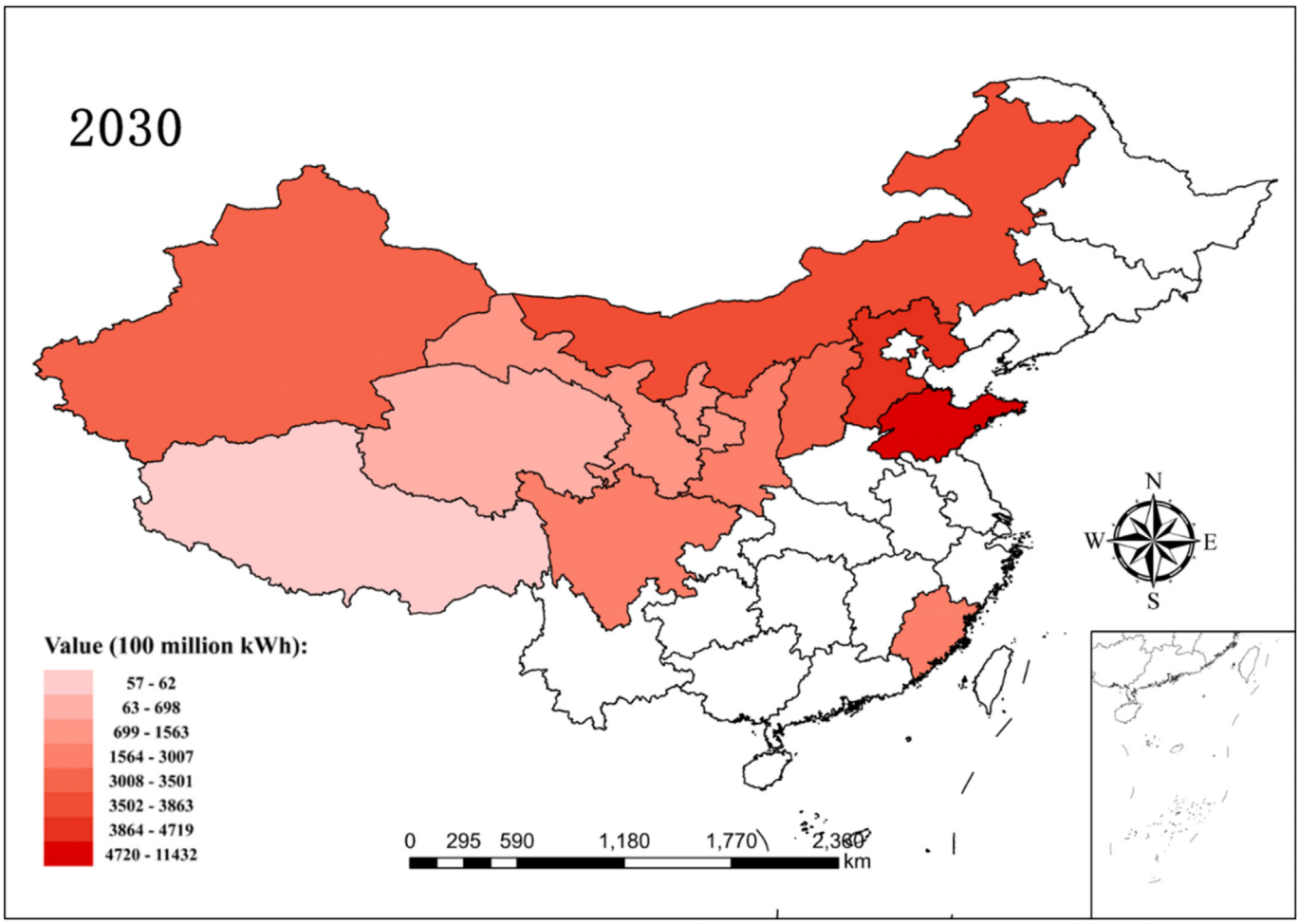

Fig. 9. Electricity consumption in 2030 in SSP1.

Table 5
The prediction of electricity consumption in 2020 and 2030 in SSP1.

Province	2020		2030		Electricity consumption increases in 2030 compared to 2020 (%)
	Electricity consumption (100 million kWh)	Proportion of electricity consumption (%)	Electricity consumption (100 million kWh)	Proportion of electricity consumption (%)	
Hebei	3518.04	13.49	4718.02	12.23	34
Shanxi	2272.93	8.72	3196.94	8.28	41
Inner Mongolia	2869.63	11.01	3862.89	10.01	35
Fujian	2281.11	8.75	2917.99	7.56	28
Shandong	6111.05	23.44	11431.33	29.62	87
Sichuan	2286.02	8.77	3006.70	7.79	32
Tibet	57.01	0.22	61.83	0.16	8
Shaanxi	1607.27	6.17	2284.23	5.92	42
Gansu	1223.09	4.69	1562.95	4.05	28
Qinghai	609.01	2.34	697.99	1.81	15
Ningxia	1028.84	3.95	1351.44	3.50	31
Xinjiang	2206.11	8.46	3500.62	9.07	59
Sum	26070.12	100	38592.93	100	48

large-scale development of arable land, they are less suitable for PV development. Therefore, it was predicted that 100% PV power generation will be far from sufficient in 2030. In contrast, in the most central and western regions of China, due to the relatively slow economic development speeds and urbanization levels, such as Ningxia and Tibet, the built-up areas were predicted to change little and the PV potential will be significant in the future.

6.2. Electricity consumption and the supply-demand comparison

Electricity consumption is closely related to population, industrial output value, and GDP. Based on the results in 4.4.2, the population, GDP value for Shandong and Hebei provinces are in the forefront of the industrial added value and in the subsequent electricity consumption prediction, they accounted for 37% and 42% of the total electricity consumption of 12 provinces in SSP1. In

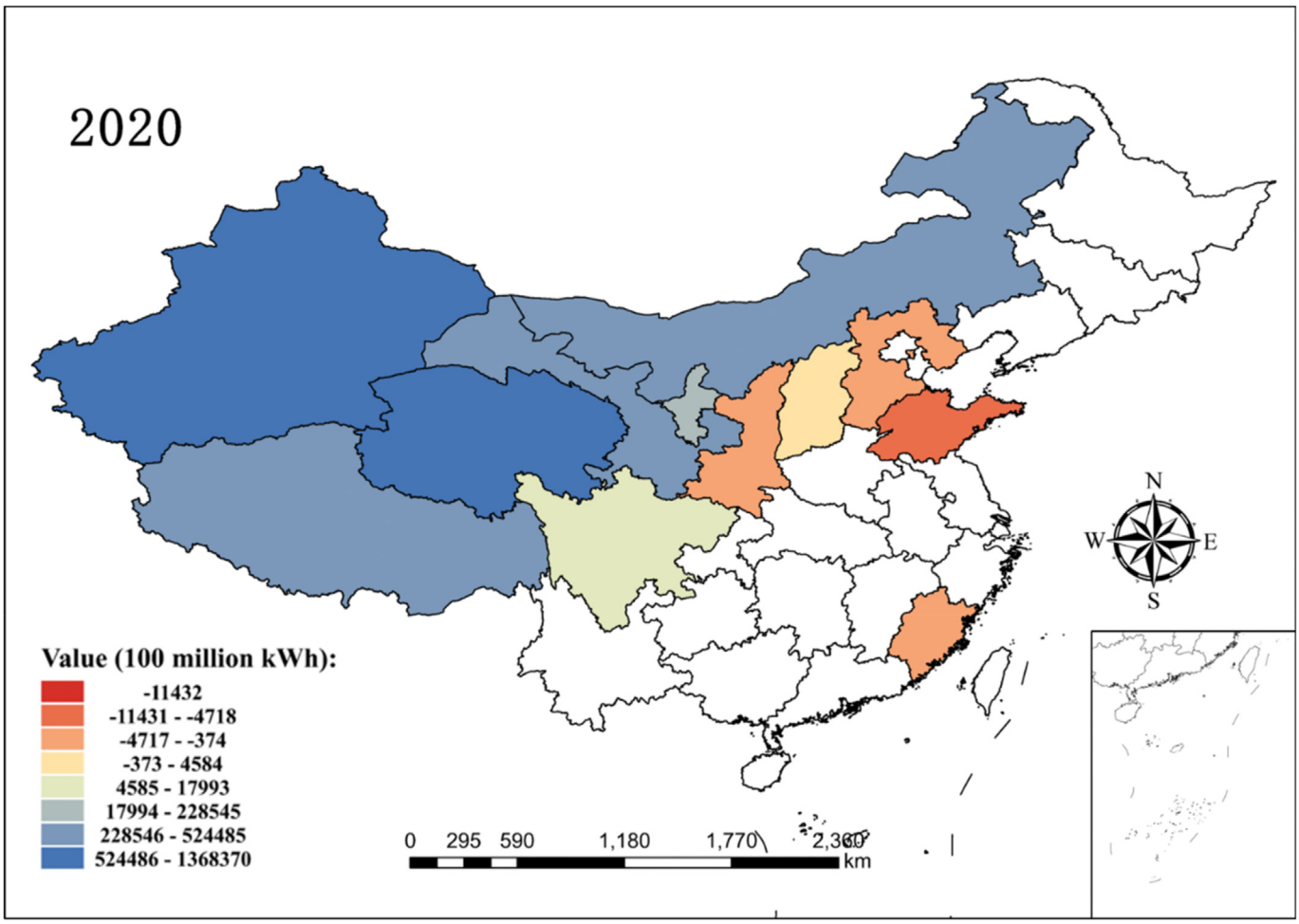

Fig. 10. The gap between supply and demand of PV power in 2020 in SSP1.

contrast, in Tibet, Qinghai and Ningxia, due to the small populations and low industrial value-added, the future predicted power consumption accounted for 7% and 8%.

The supply and demand situation displayed spatial heterogeneity. And in future, the contradiction between the less PV power generation due to the expansion of built-up areas and an increase in electricity demand will be intensified, especially in areas with rapid economic development. However, China's overall PV power generation and consumption in the future is considerable. According to the prediction of the electricity consumption of China in 2030 [36], the potential for PV power generation in the 12 provinces would be 39.8 times that of the national society in 2020 and 30.8 times in 2030. That is larger than the prediction results found in Yang et al., which showed that generation potential for large-scale PV can exceed China's national power demand in 2030 by 10.9 times [37]. That may because in this study the supply and demand of PV power from the perspective of the maximum PV power generation was compared and it is normal for the ratio to be slightly larger in 2030. In future studies on the relationship between PV supply and demand, changes in other land resource types, such as cultivated land and forest land should be considered. And more accurate data collection and calculation of PV power generation can be conducted by recording daily and monthly solar radiation data.

7. Conclusions and policy implications

To explore the impact of land resource changes on the PV generation potential under socio-economic development, the future built-up area was predicted. Based on this result, the future suitable area for PV construction and the corresponding generation potential were obtained. Finally, a forecast of the electricity consumption was compared with generation potential to better predict the supply and demand situation under a 100% PV power generation scenario. The conclusions are as follows.

(1) The impact of changes in the built-up areas on the PV construction varied in each province. Hebei, Shandong, and Fujian are expected to have almost no suitable land area for the development of centralized PV systems in 2030. The built-up area of Qinghai and Xinjiang has grown rapidly, but due to its geographical advantages, the suitable area has not changed significantly.
(2) The PV generation potential in China was found to be generally high in the western region accounting for 86% and low in the eastern region accounting for 0.01%. In Xinjiang, Qinghai, Tibet, and Inner Mongolia, the generation potential

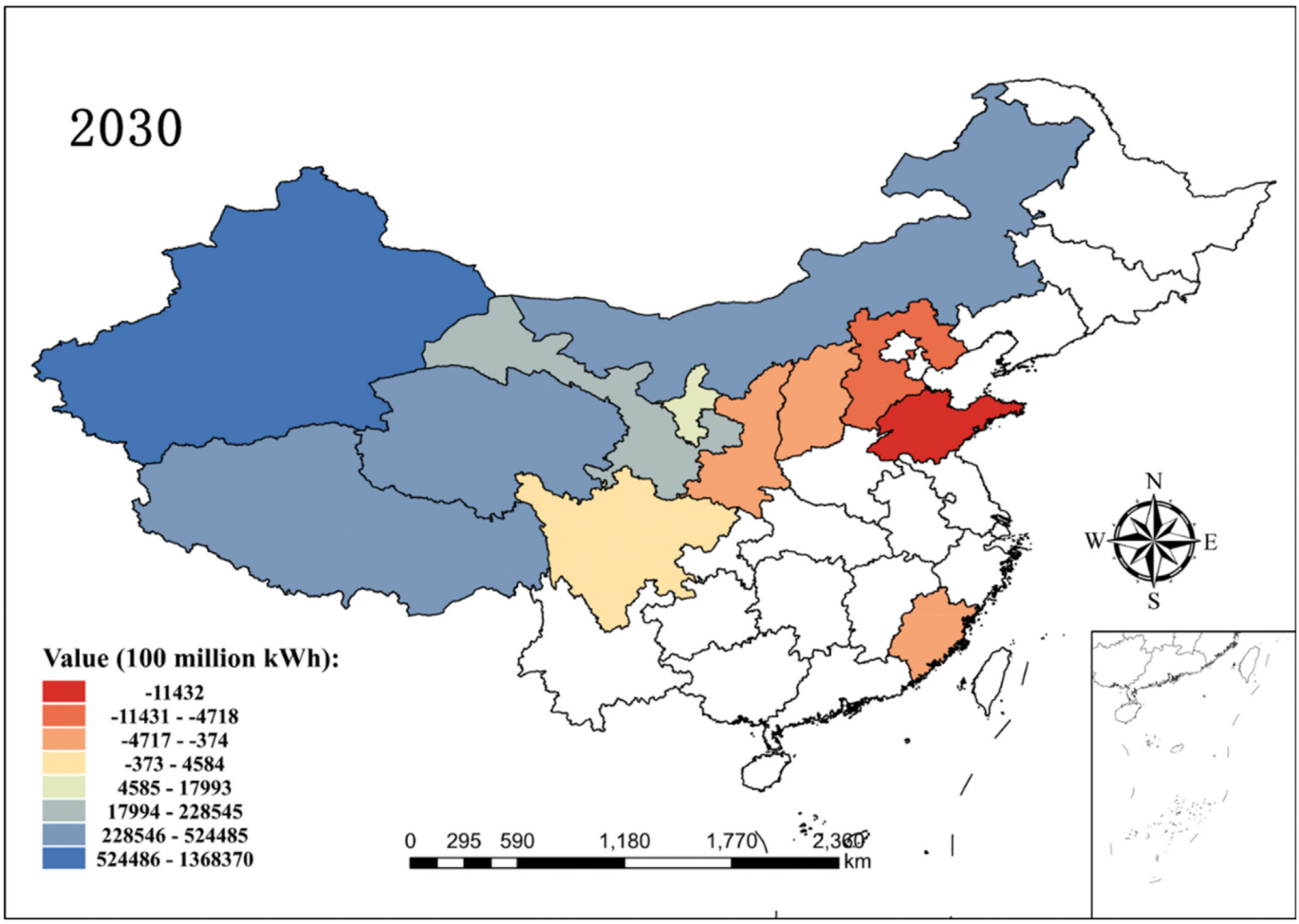

Fig. 11. The gap between supply and demand of PV power in 2030 in SSP1.

Table 6
The gap between supply and demand and the ratio in 2020 and 2030 in SSP1.

Province	2020		2030	
	The gap between supply and demand (100 million kWh)	Ratio of supply to demand	The gap between supply and demand (100 million kWh)	Ratio of supply to demand
Hebei	−3117.26	0.11	−4718.02	0
Shanxi	1226.66	1.54	−374.19	0.88
Inner Mongolia	404727.63	142.04	403660.89	105.50
Fujian	−2281.11	0	−2917.99	0
Shandong	−5994.04	0.02	−11431.33	0
Sichuan	8033.31	4.51	4583.62	2.52
Tibet	457061.71	8017.96	457032.60	7392.35
Shaanxi	−760.04	0.53	−1582.88	0.31
Gansu	229332.34	188.50	228544.96	147.23
Qinghai	524697.72	862.56	524484.16	752.42
Ningxia	18488.53	18.97	17992.05	14.31
Xinjiang	1370324.05	622.15	1368369.26	391.89

still occupies an important position in 2020 and 2030 while Fujian, Hebei, and Shandong show little PV potential.

(3) Electricity consumption was found to be larger in the eastern and northern regions and less in the western region. And the gap between the PV potential and social electricity consumption was decreasing. It was estimated that the potential for PV power generation in the 12 provinces would be 39.8 times that of the national society in 2020 and 30.8 times in 2030.

The ratio of PV supply and demand was found to be reducing from the perspective of country and province. PV generation in the future may not meet the demand for social electricity consumption. Therefore, it's significant to cooperate multiple energy distribution in future power planning. In addition, the supply and demand of PV in the region displayed significant spatial differences. PV potential areas should make full use of solar resources and strengthen power transmission facilities across provinces to solve this problem. With the reduction of suitable areas for the PV construction, the eastern

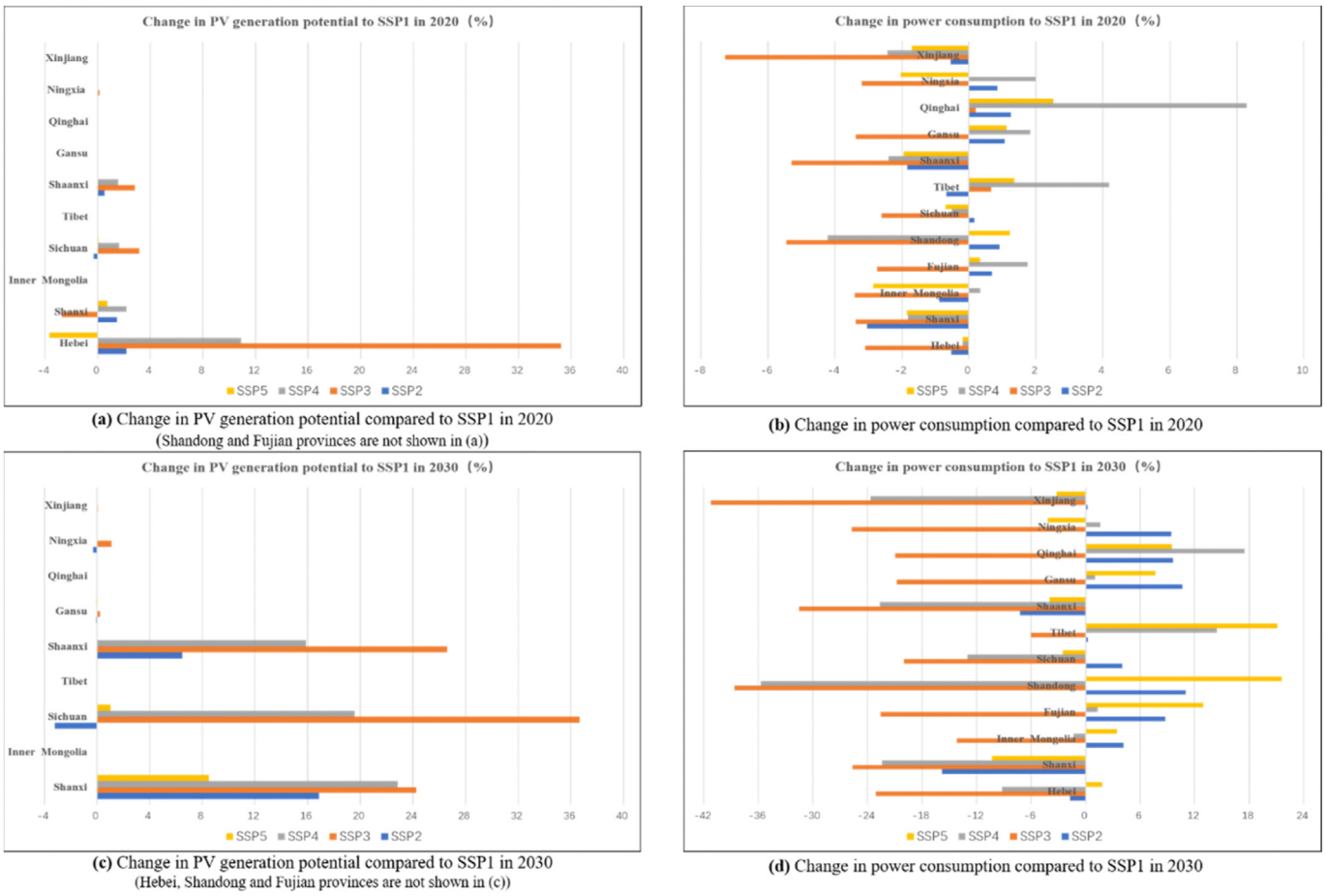

(a) Change in PV generation potential compared to SSP1 in 2020 (Shandong and Fujian provinces are not shown in (a))

(b) Change in power consumption compared to SSP1 in 2020

(c) Change in PV generation potential compared to SSP1 in 2030 (Hebei, Shandong and Fujian provinces are not shown in (c))

(d) Change in power consumption compared to SSP1 in 2030

Fig. 12. PV generation potential and power consumption in SSPs in 2020 and 2030.

region should install PV system from the perspective of more efficiently distributing PV power, which will not only reduce the spatial footprint area needed PV systems, but also achieve the goal of short-distance power transmission and a timely power supply.

Declaration of competing interest

The authors declare that they have no known competing financial interests or personal relationships that could have appeared to influence the work reported in this paper.

Acknowledgements

This work was supported by the National Natural Science Foundation of China [Grant No. 51908249], the Natural Science Foundation of the Jiangsu Higher Education Institutions of China [Grant No. 19KIB560012], the High-level Scientific Research Foundation for the introduction of talent for Jiangsu University [Grant No. 18JDG038].

Appendix A. Supplementary data

Supplementary data to this article can be found online at https://doi.org/10.1016/j.energy.2020.119611.

References

[1] Hernandez RR, Hoffacker MK, Murphy-Mariscal ML, Wu GC, Allen MF. Solar energy development impacts on land cover change and protected areas. Proc Natl Acad Sci U S A 2015;112:13579–84. https://doi.org/10.1073/pnas.1517656112.

[2] Arán Carrión J, Espín Estrella A, Aznar Dols F, Zamorano Toro M, Rodríguez M, Ramos Ridao A. Environmental decision-support systems for evaluating the carrying capacity of land areas: optimal site selection for grid-connected photovoltaic power plants. Renew Sustain Energy Rev 2008;12:2358–80. https://doi.org/10.1016/j.rser.2007.06.011.

[3] Marques AC, Fuinhas JA, Pereira DA. Have fossil fuels been substituted by renewables? An empirical assessment for 10 European countries. Energy Pol 2018;116:257–65. https://doi.org/10.1016/j.enpol.2018.02.021.

[4] Yue CD, Huang GR. An evaluation of domestic solar energy potential in Taiwan incorporating land use analysis. Energy Pol 2011;39:7988–8002. https://doi.org/10.1016/j.enpol.2011.09.054.

[5] Gunderson I, Goyette S, Gago-Silva A, Quiquerez L, Lehmann A. Climate and land-use change impacts on potential solar photovoltaic power generation in the Black Sea region. Environ Sci Pol 2015;46:70–81. https://doi.org/10.1016/j.envsci.2014.04.013.

[6] China photovoltaic power plant assets transaction white paper. Chinese version, https://www.pwccn.com/zh/deals/publications/power-plant-white-paper-2019.pdf; 2019.

[7] Yang L, Jiang J, Liu T, Li Y, Zhou Y, Gao X. Projections of future changes in solar radiation in China based on CMIP5 climate models. Glob Energy Interconnect 2018;1:452–9. https://doi.org/10.14171/j.2096-5117.gei.2018.04.005.

[8] Capellán-Pérez I, de Castro C, Arto I. Assessing vulnerabilities and limits in the transition to renewable energies: land requirements under 100% solar energy scenarios. Renew Sustain Energy Rev 2017;77:760–82. https://doi.org/10.1016/j.rser.2017.03.137.

[9] Ping L, Feng L, Hongwei W. Analysis and forecast of China's total economy and its structure from 2016–2035. Chinese J Eng Sci 2017;19:13. https://doi.org/10.15302/j-sscae-2017.01.003.

[10] Majumdar D, Pasqualetti MJ. Analysis of land availability for utility-scale power plants and assessment of solar photovoltaic development in the state of Arizona, USA. Renew Energy 2019;134:1213–31. https://doi.org/10.1016/j.renene.2018.08.064.

[11] Zhang Y, Ren J, Pu Y, Wang P. Solar energy potential assessment: a framework to integrate geographic, technological, and economic indices for a potential analysis. Renew Energy 2020;149:577–86. https://doi.org/10.1016/

j.renene.2019.12.071.
[12] Kleemann J, Baysal G, Bulley HNN, Fürst C. Assessing driving forces of land use and land cover change by a mixed-method approach in north-eastern Ghana, West Africa. J Environ Manag 2017;196:411–42. https://doi.org/10.1016/j.jenvman.2017.01.053.
[13] Jing Y, Meng LIUZ. Resources calculation of solar radiation based on matlab. 2011. https://doi.org/10.16189/j.cnki.nygc.2011.01.010.
[14] Zhe M. Solar photovoltaic optimization design and installationvol. 10; 2012. https://doi.org/10.13537/j.issn.1004-3918.2012.12.004. 3.
[15] Zhang M, Cheng CH, Ma HY. Projection of residential and commercial electricity consumption under SSPs in Jiangsu province, China. Adv Clim Change Res 2020;11:131–40. https://doi.org/10.1016/j.accre.2020.06.005.
[16] Ding Xiaojiang, Zhong Fanglei, Mao Jinhuang, Song Xiaoyu, Huang Chunlin. Prediction of the urbanization level of China's provinces under the shared social economy path. Climate Change Research 2018;14(4):392–401. https://doi:10.12006/j.issn.1673-1719.2018.018.
[17] He G, Kammen DM. Where, when and how much solar is available? A provincial-scale solar resource assessment for China. Renew Energy 2016;85:74–82. https://doi.org/10.1016/j.renene.2015.06.027.
[18] Edalat MM, Stephen H. Effects of two utility-scale solar energy plants on land-cover patterns using SMA of Thematic Mapper data. Renew Sustain Energy Rev 2017;67:1139–52. https://doi.org/10.1016/j.rser.2016.09.079.
[19] Dupraz C, Marrou H, Talbot G, Dufour L, Nogier A, Ferard Y. Combining solar photovoltaic panels and food crops for optimising land use: towards new agrivoltaic schemes. Renew Energy 2011;36:2725–32. https://doi.org/10.1016/j.renene.2011.03.005.
[20] Y wei Sun, Hof A, Wang R, Liu J, Lin Y jie, D wei Yang. GIS-based approach for potential analysis of solar PV generation at the regional scale: a case study of Fujian Province. Energy Pol 2013;58:248–59. https://doi.org/10.1016/j.enpol.2013.03.002.
[21] Suh J, Brownson JRS. Solar farm suitability using geographic information system fuzzy sets and analytic hierarchy processes: case study of Ulleung Island, Korea. Energies 2016;9. https://doi.org/10.3390/en9080648.
[22] Jiang Tong, Zhao Jing, Cao Lige, Wang Yanjun, Subuda, Cheng Jing, Wang Run, Gao Chao. Forecast of economic changes in China and its provinces under the shared social economic path. Climate Change Research 2018;14(1):50–8. https://doi:10.12006/j.issn.1673-1719.2017.161.
[23] Calvert K, Mabee W. More solar farms or more bioenergy crops? Mapping and assessing potential land-use conflicts among renewable energy technologies in eastern Ontario, Canada. Appl Geogr 2015;56:209–21. https://doi.org/10.1016/j.apgeog.2014.11.028.
[24] de Vries BJM, van Vuuren DP, Hoogwijk MM. Renewable energy sources: their global potential for the first-half of the 21st century at a global level: an integrated approach. Energy Pol 2007;35:2590–610. https://doi.org/10.1016/j.enpol.2006.09.002.
[25] Li W, Stadler S, Ramakumar R. Modeling and assessment of wind and insolation resources with a focus on their complementary nature: a case study of Oklahoma. Ann Assoc Am Geogr 2011;101:717–29. https://doi.org/10.1080/00045608.2011.567926.
[26] Shafiullah GM, Amanullah MTO, Shawkat Ali ABM, Jarvis D, Wolfs P. Prospects of renewable energy - a feasibility study in the Australian context. Renew Energy 2012;39:183–97. https://doi.org/10.1016/j.renene.2011.08.016.
[27] Nema P, Nema RK, Rangnekar S. A current and future state of art development of hybrid energy system using wind and PV-solar: a review. Renew Sustain Energy Rev 2009;13:2096–103. https://doi.org/10.1016/j.rser.2008.10.006.
[28] Noorollahi E, Fadai D, Shirazi MA, Ghodsipour SH. Land suitability analysis for solar farms exploitation using GIS and fuzzy analytic hierarchy process (FAHP) - a case study of Iran. Energies 2016;9:1–24. https://doi.org/10.3390/en9080643.
[29] Martín-Chivelet N. Photovoltaic potential and land-use estimation methodology. Energy 2016;94:233–42. https://doi.org/10.1016/j.energy.2015.10.108.
[30] Dan- ZHU. Calculation of solar radiation and generated energy on inclined plane and optimal inclined anglevol. 4; 2012. https://doi.org/10.13614/j.cnki.11-1962/tu.2012.s2.063. 8.
[31] Dong N, You L, Cai W, Li G, Lin H. Land use projections in China under global socioeconomic and emission scenarios: utilizing a scenario-based land-use change assessment framework. Global Environ Change 2018;50:164–77. https://doi.org/10.1016/j.gloenvcha.2018.04.001.
[32] Jiang Tong, Zhao Jing, Cheng Jing, Cao Lige, Wang Yanjun, Sun Hemin, Wang Anqian, Huang Jinlong, Subuda, Wang Run. Forecast of population changes in China and by provinces under the IPCC shared socio-economic path. Climate Change Research 2017;13(2):128–37. https://doi:10.12006/j.issn.1673-1719.2016.249.
[33] Pan Jinyu, Su Buda, Wang Yanjun, Jing Cheng, Zhai Jianqing, Jiang Tong. Spatio-temporal changes in China's sub-industry output value from 2020 to 2050 under shared social economic paths (SSPs). Climate Change Research. https://kns.cnki.net/kcms/detail/11.5368.p.20201014.0901.002.html.
[34] On S, Long THE, Prediction T, Annual OF, Using C, Least P, et al. Íôîãê ¥ study on the long term prediction of annual electricity consumption using partial least square regressive model. 2003. p. 17–21. https://doi.org/10.13334/j.0258-8013.pcsee.2003.10.004. 8013.
[35] 2019 photovoltaic power grid operation in China. National Energy Administration 2020. http://www.nea.gov.cn/2020-02/28/c_138827923.htm. [Accessed 28 February 2020].
[36] Tan X, Hu Z, Xu M, Shan B, Han X, Wen Q. Scenario analysis of China's electricity demand in the year 2030. An explor into China's econ dev electr demand by year 2050 2013;141. https://doi.org/10.1016/B978-0-12-420159-0.00006-0. 60.
[37] Yang Q, Huang T, Wang S, Li J, Dai S, Wright S, et al. A GIS-based high spatial resolution assessment of large-scale PV generation potential in China. Appl Energy 2019;247:254–69. https://doi.org/10.1016/j.apenergy.2019.04.005.
[38] Xu M, Xie P, Xie BC. Study of China's optimal solar photovoltaic power development path to 2050. Resour Pol 2020;65:101541. https://doi.org/10.1016/j.resourpol.2019.101541.
[39] Rachchh R, Kumar M, Tripathi B. Solar photovoltaic system design optimization by shading analysis to maximize energy generation from limited urban area. Energy Convers Manag 2016;115:244–52. https://doi.org/10.1016/j.encoman.016.02.059.
[40] Carrión JA, Espín Estrella A, Aznar Dols F, Ridao AR. The electricity production capacity of photovoltaic power plants and the selection of solar energy sites in Andalusia (Spain). Renew Energy 2008;33:545–52. https://doi.org/10.1016/j.renene.2007.05.041.
[41] Sabo ML, Mariun N, Hizam H, Mohd Radzi MA, Zakaria A. Spatial matching of large-scale grid-connected photovoltaic power generation with utility demand in Peninsular Malaysia. Appl Energy 2017;191:663–88. https://doi.org/10.1016/j.apenergy.2017.01.087.
[42] Sánchez-Lozano JM, Teruel-Solano J, Soto-Elvira PL, Socorro García-Cascales M. Geographical Information Systems (GIS) and Multi-Criteria Decision Making (MCDM) methods for the evaluation of solar farms locations: case study in south-eastern Spain. Renew Sustain Energy Rev 2013;24:544–56. https://doi.org/10.1016/j.rser.2013.03.019.
[43] China National Energy Administration. The 13th five-year plan for solar energy development. 2016. China.